

# Vecchia approximations of Gaussian-process predictions

Matthias Katzfuss<sup>\*†</sup>    Joseph Guinness<sup>‡</sup>    Wenlong Gong<sup>\*</sup>

## Abstract

Gaussian processes (GPs) are highly flexible function estimators used for geospatial analysis, nonparametric regression, and machine learning, but they are computationally infeasible for large datasets. Vecchia approximations of GPs have been used to enable fast evaluation of the likelihood for parameter inference. Here, we study Vecchia approximations of spatial predictions at observed and unobserved locations, including obtaining joint predictive distributions at large sets of locations. We propose a general Vecchia framework for GP predictions, which contains some novel and some existing special cases. We study the accuracy and computational properties of these approaches theoretically and numerically. We show that our new approaches exhibit linear computational complexity in the total number of spatial locations. We also apply our methods to a satellite dataset of chlorophyll fluorescence.

**Keywords:** computational complexity; kriging; large datasets; sparsity; spatial statistics

## 1 Introduction

Gaussian processes (GPs) are popular models for functions, time series, and spatial fields, with a myriad of application areas such as geospatial analysis (e.g., Banerjee et al., 2004; Cressie and Wikle, 2011), nonparametric regression and machine learning (e.g., Rasmussen and Williams, 2006), and the analysis of computer experiments (e.g., Kennedy and O’Hagan, 2001). GPs are flexible, interpretable, allow natural probabilistic quantification of uncertainty, and are thus well-suited for big-data applications in principle. However, direct application of GPs incurs computational cost that is cubic in the data size, which is too expensive for many modern datasets of interest.

To deal with this computational problem, numerous GP approximations or simplifying assumptions have been proposed. These include imposing sparsity on covariance matrices (Furrer et al., 2006; Kaufman et al., 2008; Du et al., 2009), sparsity on precision matrices (Rue and Held, 2005; Lindgren et al., 2011; Nychka et al., 2015), and low-rank structure (e.g., Higdon, 1998; Wikle and Cressie, 1999; Quiñonero-Candela and Rasmussen, 2005; Banerjee et al., 2008; Cressie and Johannesson, 2008; Katzfuss and Cressie, 2011; Tzeng and Huang, 2018). While low-rank approaches are poorly suited for capturing fine-scale dependence,

---

<sup>\*</sup>Department of Statistics, Texas A&M University

<sup>†</sup>Corresponding author: [katzfuss@gmail.com](mailto:katzfuss@gmail.com)

<sup>‡</sup>Department of Biological Statistics and Computational Biology and Department of Statistical Science, Cornell University

sparsity-based approaches can generally not guarantee linear scaling in the data or grid size, especially in higher dimensions.

We focus on Vecchia approximations, which obtain a sparse Cholesky factor of the precision matrix by removing conditioning variables in a factorization of the joint density of the GP observations into a product of conditional distributions (Vecchia, 1988; Stein et al., 2004; Guinness, 2018; Sun and Stein, 2016). For the typical setting of GP observations that include additive noise, Katzfuss and Guinness (2017) consider a general Vecchia framework that applies the Vecchia approximation to a vector consisting of both the latent GP realizations and the noisy data. This framework contains many other popular GP approximations as special cases (e.g., Snelson and Ghahramani, 2007; Sang et al., 2011; Finley et al., 2009; Datta et al., 2016; Katzfuss, 2017; Katzfuss and Gong, 2017).

So far, most Vecchia approaches have solely or primarily been concerned with approximations of the likelihood for parameter inference. We consider instead the use of Vecchia approximations for obtaining marginal and joint spatial predictions at observed and unobserved locations. Joint predictive distributions are crucial for accurate uncertainty quantification for spatial averages or totals. For example, climate scientists are interested in obtaining uncertainties on the global average temperature, and hydrologists may wish to quantify uncertainty in total rainfall in a catchment area.

The literature on GP prediction, also referred to as kriging, using Vecchia approximations is sparse. Guinness (2018) considers prediction using conditional expectation and uncertainty quantification using conditional simulations in a Vecchia approach based solely on conditioning on observed variables. This is relatively computationally cheap, but uncertainty measures contain random simulation error, and the observed conditioning might not provide accurate approximations in the presence of noise (Katzfuss and Guinness, 2017). Datta et al. (2016) consider a fully latent Vecchia approach that can be used for prediction, but it does not guarantee linear complexity and it relies on the assumption that process evaluations at unobserved locations are conditionally independent given the process at the observed locations. A further example in which Vecchia has essentially been used for prediction is the exact iterative solver with a Vecchia pre-conditioner considered in Stroud et al. (2017), but this approach is feasible only if prediction is desired at a small number of locations.

Whereas Katzfuss and Guinness (2017) focused on a general Vecchia framework for approximating the likelihood function, here we extend the framework to obtain computational approximations for the purpose of spatial prediction, considering the effects of the choice of ordering and conditioning rules on the approximation accuracy of the predictive distribution in various scenarios. We introduce novel approaches within the framework, for which we can guarantee high levels of sparsity for the matrices necessary for inference. The resulting time complexity for inference is thus guaranteed to be linear in the number of data points and prediction locations. In addition, we use the framework to synthesize the existing literature.

This article is organized as follows. Section 2 reviews GP prediction. In Section 3, we introduce general Vecchia approximations of GP prediction. In Sections 4 and 5, we discuss specific examples. In Section 6, we summarize the approaches and study their properties. Sections 7 and 8 provide numerical comparisons using simulated and real data, respectively. We conclude in Section 9. Appendices A–C contain further details and proofs. The methods and algorithms proposed here are implemented in the R package `GPvecchia` available at <https://github.com/katzfuss-group/GPvecchia>.

## 2 Gaussian processes and prediction

The process of interest is denoted by  $\{y(\mathbf{s}) : \mathbf{s} \in \mathbb{D}\}$ , or  $y(\cdot)$ , on a continuous (i.e., non-gridded) domain  $\mathbb{D} \subset \mathbb{R}^d$ ,  $d \in \mathbb{N}^+$ . We assume that  $y(\cdot) \sim GP(0, K)$  is a Gaussian process (GP) with mean zero and covariance function  $K : \mathbb{D} \times \mathbb{D} \rightarrow \mathbb{R}$ , which is assumed known up to some parameters. Let  $\mathbf{s}_i \in \mathbb{D}$  for  $i = 1, \dots, n$ , and define the location vector  $\mathcal{S} = (\mathbf{s}_1, \dots, \mathbf{s}_n)$ . For simplicity, we assume throughout that the locations in  $\mathcal{S}$  are unique. Define  $y_i = y(\mathbf{s}_i)$  and the vectors  $\mathbf{y} = (y_1, \dots, y_n)$  and  $\mathbf{z} = (z_1, \dots, z_n)$ . The response variables  $z_i$  are noisy versions of latent  $y_i$ :  $z_i | \mathbf{y} \sim \mathcal{N}(y_i, \tau_i^2)$  independently for all  $i$ . Thus, the covariance matrix of  $\mathbf{y}$  is  $\mathbf{K} = K(\mathcal{S}, \mathcal{S})$ , and the covariance matrix of  $\mathbf{z}$  is  $\mathbf{C} = \mathbf{K} + \mathbf{D}$ , where  $\mathbf{D}$  is a diagonal matrix containing the noise or nugget variances,  $\mathbf{D}_{ii} = \tau_i^2$ . Define the index vector  $o \subset (1, \dots, n)$  of length  $n_o = |o|$  such that the subvector  $\mathbf{z}_o$  contains all observed response variables, and  $\mathcal{S}_o$  represents the vector of observed locations. (We use the vector and indexing notation described in Katzfuss and Guinness (2017, App. A).) We also define  $p = (1, \dots, n) \setminus o$  to be an index vector of length  $n_p = |p| = n - n_o$ , such that  $\mathcal{S}_p$  is the vector of unobserved (prediction) locations. For clarification, this terminology is summarized in Table 1. Inference on unknown parameters  $\boldsymbol{\theta}$  in  $K$  and  $\tau_i^2$  can be carried out based on the multivariate normal likelihood,  $f(\mathbf{z}_o) = \mathcal{N}_{n_o}(\mathbf{z}_o | \mathbf{0}, \mathbf{C}_{oo})$ .

The goal for prediction is to obtain the posterior predictive distribution of  $\mathbf{y}$  via

$$f(\mathbf{y} | \mathbf{z}_o) = \int f(\mathbf{y} | \mathbf{z}_o, \boldsymbol{\theta}) dF(\boldsymbol{\theta} | \mathbf{z}_o). \quad (1)$$

The density  $f(\mathbf{y} | \mathbf{z}_o, \boldsymbol{\theta})$  is normal with mean  $\boldsymbol{\mu}(\boldsymbol{\theta}) = \mathbf{K}_{\bullet o} \mathbf{C}_{oo}^{-1} \mathbf{z}_o$  and covariance matrix

$$\boldsymbol{\Sigma}(\boldsymbol{\theta}) = \mathbf{K} - \mathbf{K}_{\bullet o} \mathbf{C}_{oo}^{-1} \mathbf{K}_{o\bullet}, \quad (2)$$

where  $\mathbf{K}$  and  $\mathbf{C}$  implicitly depend on  $\boldsymbol{\theta}$ . When using maximum-likelihood estimation, the posterior distribution  $F(\boldsymbol{\theta} | \mathbf{z}_o)$  of the parameters is effectively approximated by a point mass at  $\boldsymbol{\theta} = \hat{\boldsymbol{\theta}}$  in (1), and so  $f(\mathbf{y} | \mathbf{z}_o) = \mathcal{N}(\mathbf{y} | \boldsymbol{\mu}(\hat{\boldsymbol{\theta}}), \boldsymbol{\Sigma}(\hat{\boldsymbol{\theta}}))$ . For Bayesian inference using MCMC, the parameter posterior in (1) is approximated as discrete uniform on, say,  $\boldsymbol{\theta}^{(1)}, \dots, \boldsymbol{\theta}^{(L)}$ , and so  $f(\mathbf{y} | \mathbf{z}_o) = (1/L) \sum_l \mathcal{N}(\mathbf{y} | \boldsymbol{\mu}(\boldsymbol{\theta}^{(l)}), \boldsymbol{\Sigma}(\boldsymbol{\theta}^{(l)}))$ . Therefore, GP prediction requires obtaining  $f(\mathbf{y} | \mathbf{z}_o, \boldsymbol{\theta}) = \mathcal{N}(\mathbf{y} | \boldsymbol{\mu}(\boldsymbol{\theta}), \boldsymbol{\Sigma}(\boldsymbol{\theta}))$  for particular fixed values of  $\boldsymbol{\theta}$ . Here and in the following, we will thus suppress dependence on  $\boldsymbol{\theta}$  and regard it as fixed and known, unless stated otherwise. Sometimes (e.g., for cross validation), interest might also be in predicting  $\mathbf{z}_p$ , but this is a trivial extension of predicting  $\mathbf{y}_p$ , in that  $\mathbf{z}_p | \mathbf{z}_o \sim \mathcal{N}(\boldsymbol{\mu}_p, \boldsymbol{\Sigma}_{pp} + \mathbf{D}_{pp})$ .

While GP prediction is mathematically straightforward, it can be computationally expensive. The time complexity for obtaining the entire matrix  $\boldsymbol{\Sigma}$  in (2) is  $\mathcal{O}(n_o^3 + nn_o^2 + n^2 n_o)$ , and even just obtaining its diagonal elements (i.e., the prediction variances) requires  $\mathcal{O}(n_o^3 + nn_o^2)$  time. Thus, GP prediction is computationally infeasible for large  $n_o$  or  $n$ , and approximations or simplifying assumptions are necessary.

Notation	Terminology
$o \subset (1, \dots, n)$	vector of indices of <b>observed</b> locations
$p = (1, \dots, n) \setminus o$	vector of indices of (unobserved) <b>prediction</b> locations
$\mathbf{y}, \mathbf{y}_o, \mathbf{y}_p$	vectors of <b>latent</b> variables
$\mathbf{z}, \mathbf{z}_o, \mathbf{z}_p$	vectors of <b>response</b> variables

Table 1: Summary of terminology

### 3 GP prediction using Vecchia approximations

We now present a general framework for Vecchia approximations of GP predictions, which is an extension of the general Vecchia framework introduced in Katzfuss and Guinness (2017). (While they allowed splitting the locations into small groups, we consider only the case of groups of size 1 here for ease of exposition.) Recall  $\mathcal{S} = (\mathbf{s}_1, \dots, \mathbf{s}_n)$  is an ordered vector of locations, and so implicitly, one has made a decision about how to order the unordered *set* of locations  $\{\mathbf{s}_1, \dots, \mathbf{s}_n\}$ . The vector of GP realizations,  $\mathbf{y}$ , is ordered according to  $\mathcal{S}$ , because  $y_i = y(\mathbf{s}_i)$ . Further, let  $\mathbf{x} = \mathbf{y} \cup \mathbf{z}_o$  with ordering defined via an index function  $\#$  that returns the index that an element occupies in a vector:  $\#(y_i, \mathbf{x}) < \#(y_j, \mathbf{x})$  if  $i < j$  (i.e.,  $\mathbf{y}$  retains its relative ordering), and  $\#(z_i, \mathbf{x}) = \#(y_i, \mathbf{x}) + 1$  if  $i \in o$  (i.e.,  $z_i$  is ordered directly after  $y_i$ ). Simply speaking,  $\mathbf{x}$  is formed by inserting the elements of  $\mathbf{z}_o$  directly after their corresponding elements in  $\mathbf{y}$ .

#### 3.1 The general Vecchia approximation

Applying the general Vecchia approximation (Katzfuss and Guinness, 2017) to  $\mathbf{x}$ , we obtain

$$\widehat{f}(\mathbf{x}) = \left( \prod_{i=1}^n f(y_i | \mathbf{y}_{q_y(i)}, \mathbf{z}_{q_z(i)}) \right) \left( \prod_{i \in o} f(z_i | y_i) \right), \quad (3)$$

where  $q(i) = q_y(i) \cup q_z(i)$  with  $q(i) \subset (1, \dots, i-1)$  is the conditioning index vector of size  $|q(i)| \leq m$ . The general Vecchia approximation is motivated by the exact factorization  $f(\mathbf{x}) = \prod_{j=1}^{n+n_o} f(x_j | x_1, \dots, x_{j-1})$ , but in (3) we only use a small subset of the conditioning set on the right-hand side: If  $x_j = z_i$ , we only condition on  $y_i$ , because  $z_i$  is conditionally independent of all other variables in  $\mathbf{y}$  and  $\mathbf{z}$  given  $y_i$ . If  $x_j = y_i$ , we condition on  $\mathbf{y}_{q_y(i)}$  and  $\mathbf{z}_{q_z(i)}$ , where we assume  $q_y(i) \cap q_z(i) = \emptyset$ , due to conditional independence of  $y_i$  and  $z_k$  given  $y_k$ . Thus, the approximation quality depends entirely on the choice of the ordering of  $(\mathbf{s}_1, \dots, \mathbf{s}_n)$  in  $\mathcal{S}$ , and the specification of the latent and response conditioning index vectors  $q_y(i)$  and  $q_z(i)$ , respectively, for each  $i$ . This paper is devoted to studying how these choices affect the quality of the approximation, in order to improve Vecchia’s approximation as a computationally efficient tool for spatial prediction. As shown in Katzfuss and Guinness (2017), there is a trade-off in conditioning on latent versus response variables, in that it is typically more accurate but also more computationally expensive to condition on  $y_k$  rather than on  $z_k$ . In the prediction setting considered here, we have the added restriction that  $q_z(i) \cap p = \emptyset$ , because  $\mathbf{z}_p$  is not included in  $\mathbf{x}$ . If  $q_y(i) = (1, \dots, i-1)$ , the exact distribution is recovered (i.e., then  $\widehat{f}(\mathbf{x}) = f(\mathbf{x})$ ). However, large conditioning sets negate the computational advantages, and thus the case of small  $m \ll n$  is of interest here.

#### 3.2 Matrix representations for inference

The joint distribution implied by the approximation in (3) is multivariate normal,  $\widehat{f}(\mathbf{x}) = \mathcal{N}(\mathbf{0}, \mathbf{Q}^{-1})$ , where  $\mathbf{Q} = \mathbf{U}\mathbf{U}'$ , and  $\mathbf{U}$  is the upper-triangular Cholesky factor based on a reverse row-column ordering of  $\mathbf{Q}$  (Katzfuss and Guinness, 2017, Prop. 1). We write this as  $\mathbf{U} = \text{rchol}(\mathbf{Q}) = \text{rev}(\text{chol}(\text{rev}(\mathbf{Q})))$ , where  $\text{rev}(\cdot)$  reverse-orders the rows and columns of its matrix argument, and  $\text{chol}(\cdot)$  computes the standard lower-triangular Cholesky factor.

In practice, there is no need to construct the matrix  $\mathbf{Q}$ ; rather, we compute the nonzero entries of  $\mathbf{U}$  directly via the methods outlined in Appendix A. From the expressions in Appendix A, it is easy to see that  $\mathbf{U}$  is sparse with at most  $m$  off-diagonal nonzero entries per column, and  $\mathbf{U}$  can be computed in  $\mathcal{O}(nm^3)$  time.

Given  $\mathbf{U}$ , define the submatrices  $\mathbf{A} = \mathbf{U}_{\#(\mathbf{y}, \mathbf{x}) \bullet}$  and  $\mathbf{B} = \mathbf{U}_{\#(\mathbf{z}_o, \mathbf{x}) \bullet}$  consisting of the rows of  $\mathbf{U}$  corresponding to  $\mathbf{y}$  and  $\mathbf{z}_o$ , respectively. Further, we define  $\mathbf{W} = \mathbf{Q}_{\#(\mathbf{y}, \mathbf{x}), \#(\mathbf{y}, \mathbf{x})}$  to be the submatrix of  $\mathbf{Q}$  corresponding to  $\mathbf{y}$ , which can be computed as  $\mathbf{W} = \mathbf{A}\mathbf{A}'$ . Finally, define  $\mathbf{V} = \text{rchol}(\mathbf{W})$ , so that  $\mathbf{W} = \mathbf{V}\mathbf{V}'$ .

### 3.3 Likelihood approximation

Likelihood approximation for parameter inference is discussed in detail in Katzfuss and Guinness (2017). For completeness, we briefly mention it here as well. Based on  $\mathbf{U}$  (which implicitly depends on parameters  $\boldsymbol{\theta}$ ) and the matrices calculated from it, we can evaluate the likelihood to carry out parameter inference. Integration of  $\hat{f}(\mathbf{x})$  in (3) with respect to  $\mathbf{y}$  results in the following approximate likelihood (Katzfuss and Guinness, 2017, Prop. 2):

$$-2 \log \hat{f}(\mathbf{z}_o) = -2 \sum_i \log \mathbf{U}_{ii} + 2 \sum_i \log \mathbf{V}_{ii} + \mathbf{z}_o' \mathbf{B} \mathbf{B}' \mathbf{z}_o - (\mathbf{V}^{-1} \mathbf{A} \mathbf{B}' \mathbf{z}_o)' (\mathbf{V}^{-1} \mathbf{A} \mathbf{B}' \mathbf{z}_o) + n \log(2\pi). \quad (4)$$

The computational cost for evaluating this likelihood approximation is often low, and Katzfuss and Guinness (2017) provide conditions on the  $q_y(i)$  under which the cost is guaranteed to be linear in  $n$ .

### 3.4 General Vecchia predictions

The goal for GP prediction is to obtain the posterior predictive distribution of  $\mathbf{y}$  given the response  $\mathbf{z}_o$ , or certain summaries of this distribution. General Vecchia prediction approximates the exact conditional distribution  $f(\mathbf{y}|\mathbf{z}_o)$  with the distribution implied by (3):

$$\hat{f}(\mathbf{y}|\mathbf{z}_o) = \frac{\hat{f}(\mathbf{x})}{\int \hat{f}(\mathbf{x}) d\mathbf{y}} =: \mathcal{N}_n(\boldsymbol{\mu}, \boldsymbol{\Sigma}).$$

As  $\mathbf{Q} = \mathbf{U}\mathbf{U}'$  represents the precision matrix of  $\mathbf{x} = \mathbf{y} \cup \mathbf{z}_o$ , it is a well-known property of precision matrices that  $\boldsymbol{\Sigma} = \mathbf{W}^{-1}$ , where  $\mathbf{W}$  is the submatrix of  $\mathbf{Q}$  defined in Section 3.2. While the precision matrix  $\mathbf{W}$  is sparse, the covariance matrix  $\boldsymbol{\Sigma}$  will generally be a dense  $n \times n$  matrix. Thus, it is infeasible to actually compute and store this entire matrix when  $n$  is large. The following tasks are often of interest in the context of prediction:

1. The posterior mean of  $\mathbf{y}$ , also called the kriging predictor, can be calculated as  $\boldsymbol{\mu} = -(\mathbf{V}')^{-1} \mathbf{V}^{-1} \mathbf{A} \mathbf{B}' \mathbf{z}_o$ , following Katzfuss and Guinness (2017, proof of Prop. 2).
2. The prediction variances are given by  $\text{diag}(\boldsymbol{\Sigma})$ . Based on  $\mathbf{V}$ , a selected inversion algorithm, also referred to as the Takahashi recursions (Erisman and Tinney, 1975; Li et al., 2008; Lin et al., 2011), can be used to compute  $\boldsymbol{\Sigma}_{ij}$  for all pairs  $i, j$  with  $\mathbf{W}_{ij} \neq 0$ . Thus, it also returns the prediction variances  $\boldsymbol{\Sigma}_{ii}$ .

3. The joint posterior distribution of a set of  $\ell$ , say, linear combinations is given by:  $\mathbf{Hy}|\mathbf{z}_o \sim \mathcal{N}_\ell(\mathbf{H}\boldsymbol{\mu}, (\mathbf{V}^{-1}\mathbf{H}')'(\mathbf{V}^{-1}\mathbf{H}'))$ , where  $\mathbf{H}$  is  $\ell \times n$ . As  $\mathbf{V}^{-1}\mathbf{H}'$  is generally dense, only a moderate number of linear combinations is computationally feasible. (Note that for the multi-resolution approximation (Katzfuss, 2017; Katzfuss and Gong, 2017), which is a special case of general Vecchia,  $\mathbf{V}^{-1}$  has the same sparsity as  $\mathbf{V}$ , and so  $\mathbf{V}^{-1}\mathbf{H}'$  is generally sparse if  $\mathbf{H}$  is sparse.) The variances of linear combinations can be computed faster, as  $\text{diag}(\text{var}(\mathbf{Hy}|\mathbf{z}_o)) = ((\mathbf{V}^{-1}\mathbf{H}') \circ (\mathbf{V}^{-1}\mathbf{H}'))'\mathbf{1}_n$ , where  $\circ$  denotes element-wise multiplication and  $\mathbf{1}_n$  is an  $n$ -vector of ones. The subvector  $\mathbf{y}_p = \mathbf{Hy}$  is also a linear combination with  $\mathbf{H} = \mathbf{I}_{p\bullet}$ , where  $\mathbf{I}$  is the  $n \times n$  identity matrix. Thus,  $\mathbf{y}_p|\mathbf{z}_o \sim \mathcal{N}_{n_p}(\boldsymbol{\mu}_p, (\mathbf{V}^{-1}\mathbf{I}_{\bullet p})'(\mathbf{V}^{-1}\mathbf{I}_{\bullet p}))$ .
4. For conditional simulation from the posterior predictive distribution, we can draw  $n$  samples  $a_i \stackrel{iid}{\sim} \mathcal{N}(0, 1)$  from the standard normal distribution, set  $\mathbf{a} = (a_1, \dots, a_n)'$  and  $\mathbf{y}^* = \boldsymbol{\mu} + (\mathbf{V}')^{-1}\mathbf{a} \sim \mathcal{N}(\boldsymbol{\mu}, \boldsymbol{\Sigma})$ .

All of these tasks require computation of  $\mathbf{V}$  from  $\mathbf{U}$ . As mentioned in Section 3.2,  $\mathbf{U}$  is sparse with at most  $m$  off-diagonal nonzero entries per column, which can be computed in  $\mathcal{O}(nm^3)$  time. Determining the cost of computing  $\mathbf{V} = \text{rchol}(\mathbf{W})$  is more complicated. It depends on the number of nonzero entries per column in  $\mathbf{V}$ . In general, it is crucial for fast predictions for large  $n$  that  $\mathbf{V}$  is sufficiently sparse. Computational complexity is discussed in Section 6.2 in more detail.

## 4 Latent autoregressive prediction (LAP)

Latent autoregressive prediction is obtained as a special case of the general Vecchia predictions described in Section 3, in which each  $y_i$  simply conditions on  $(y_{i-m}, \dots, y_{i-1})$ ; more precisely, we set  $q_y(i) = \{\max(1, i-m), \dots, i-1\}$  and  $q_z(i) = \emptyset$ . This amounts to a latent autoregressive process of order  $m$ .

LAP conditioning ensures that  $\mathbf{V}$  has at most  $m$  nonzero off-diagonal elements per column. This can be shown using Katzfuss and Guinness (2017, Prop. 6) by verifying that for any  $i = 1, \dots, n$ , the set  $q_y(i)$  satisfies the restriction that any pair  $j < k$  can only both be in  $q_y(i)$  if  $j \in q_y(k)$ . This restriction is satisfied here:

$$j, k \in q_y(i) \text{ with } j < k \quad \Rightarrow \quad i - m \leq j < k < i \quad \Rightarrow \quad k - m < j < k \quad \Rightarrow \quad j \in q_y(k).$$

### 4.1 LAP based on left-to-right ordering (LAPLR)

Latent autoregressive prediction is most appropriate when successive locations in  $\mathcal{S}$  (and hence variables in  $\mathbf{x}$ ) tend to be close in space, so that  $\mathbf{y}_{q_y(i)}$  has strong correlation with  $y_i$ . This is often the case with coordinate-based ordering, especially in one-dimensional space. Therefore, we only consider LAP based on left-to-right ordering (LAPLR) in  $\mathbb{D} \subset \mathbb{R}$  here.

This approach can lead to highly accurate approximations if  $m$  is chosen appropriately. For example, a GP with exponential covariance function in one dimension is a Markov process, and so we can obtain an exact representation of the joint distribution of  $\mathbf{x}$  with  $m \geq 1$ ; that is, we then have  $\hat{f}(\mathbf{x}) = f(\mathbf{x})$  and hence  $\hat{f}(\mathbf{y}|\mathbf{z}_o) = f(\mathbf{y}|\mathbf{z}_o)$ . More generally, for

a GP with Matérn covariance with smoothness  $\nu$ , we obtain nearly exact representations if  $m > \nu$  (cf. Katzfuss and Guinness, 2017, Fig. 2a).

Strictly speaking, this approach has the undesirable property that changing  $\mathcal{S}$  (e.g., by adding prediction locations) might change the joint distribution of the corresponding variables  $\mathbf{x}$ . However, as shown in Figure 1 and the numerical experiments in Section 7.1, the LAPLR approximation is so accurate that, even for small  $m$ , there is virtually no difference to the exact GP, and so all joint distributions are basically identical to the true ones.

## 5 Ordering the prediction variables last

We now consider several special cases of the general Vecchia predictions described in Section 3, which all order the observed locations first and prediction locations last; that is,  $o = (1, \dots, n_O)$  and  $p = (n_O + 1, \dots, n)$ . We refer to this approach as obs–pred ordering. We define  $q_y^o(i) = q_y(i) \cap o$  and  $q_y^p(i) = q_y(i) \cap p$  as the subvectors of the  $i$ th latent conditioning index vector corresponding to the observed and unobserved locations, respectively.

Obs–pred ordering, of course, restricts the choice of ordering in  $\mathcal{S}$  somewhat. In one dimension, we recommend separate coordinate orderings for the observed and prediction locations. In two or more dimensions, we recommend an extension of maximum–minimum distance (maxmin) ordering (Guinness, 2018) that enforces the constraint of ordering prediction locations last. For simplicity, each conditioning set  $q(i)$  will consist of the indices corresponding to the  $m$  nearest previously ordered locations (i.e., from among  $(\mathbf{s}_1, \dots, \mathbf{s}_{i-1})$ ), potentially under additional restrictions.

One advantage of obs–pred ordering is that the likelihood is unchanged when  $\mathbf{y}_p$  is removed from  $\mathbf{x}$ , resulting in  $\mathbf{x}_{\tilde{o}} = \mathbf{x} \setminus \mathbf{y}_p$ , where  $\tilde{o} = \#(\mathbf{x} \setminus \mathbf{y}_p, \mathbf{x}) = (1, \dots, 2n_O)$ :

$$\hat{f}(\mathbf{z}_o) = \int \int \hat{f}(\mathbf{x}_{\tilde{o}}) \hat{f}(\mathbf{y}_p | \mathbf{x}_{\tilde{o}}) d\mathbf{y}_p d\mathbf{y}_o = \int \hat{f}(\mathbf{x}_{\tilde{o}}) \int \hat{f}(\mathbf{y}_p | \mathbf{x}_{\tilde{o}}) d\mathbf{y}_p d\mathbf{y}_o = \int \hat{f}(\mathbf{x}_{\tilde{o}}) d\mathbf{y}_o.$$

Thus, likelihood inference can first be carried out based on  $\mathbf{x}_{\tilde{o}}$  (i.e., only based on  $\mathbf{y}_o$  and  $\mathbf{z}_o$ ) using (4) as described in Katzfuss and Guinness (2017). Then,  $\mathbf{y}_p$  can be appended at the end of  $\mathbf{x}$  when predictions are desired, without changing the distribution  $\hat{f}(\mathbf{z}_o)$ . In this way, parameter inference and prediction are carried out in a consistent framework. If  $\mathbf{U}$  has already been calculated for  $\mathbf{x}_{\tilde{o}}$ , it is also possible to reuse this matrix and simply append to it the columns corresponding to  $\mathbf{y}_p$ .

A second advantage of obs–pred ordering is that a new expression for  $\mathbf{V} = \text{rchol}(\mathbf{W})$  can be obtained. Remember that  $\mathbf{W} = \mathbf{A}\mathbf{A}'$ , and define  $\tilde{p} = \#(\mathbf{y}_p, \mathbf{x}) = (2n_O + 1, \dots, 2n_O + n_P)$ . The matrix  $\mathbf{A}$  can be written as a block matrix of the form

$$\mathbf{A} = \begin{pmatrix} \mathbf{A}_{o\tilde{o}} & \mathbf{A}_{o\tilde{p}} \\ \mathbf{0} & \mathbf{A}_{p\tilde{p}} \end{pmatrix}, \quad (5)$$

where  $\mathbf{A}_{p\tilde{p}}$  is an  $n_P \times n_P$  upper-triangular matrix.

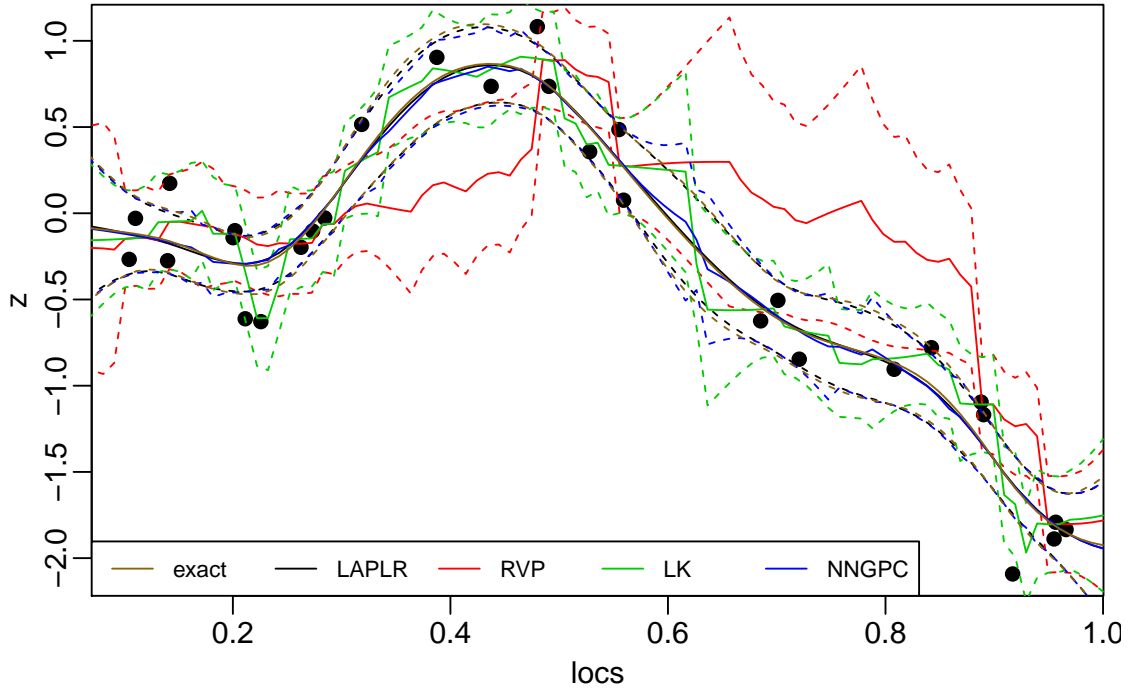
PROPOSITION 1. *Under obs–pred ordering,  $\mathbf{V} = \text{rchol}(\mathbf{W})$  can be written as*

$$\mathbf{V} = \begin{pmatrix} \mathbf{V}_{oo} & \mathbf{A}_{o\tilde{p}} \\ \mathbf{0} & \mathbf{A}_{p\tilde{p}} \end{pmatrix}, \quad (6)$$

where  $\mathbf{V}_{oo} = \text{rchol}(\mathbf{A}_{o\tilde{o}}\mathbf{A}'_{o\tilde{o}})$ .

Method	Section	obs-pred	obs cond	pred cond	linear	new
LAPLR	4.1	no	latent	yes	yes	yes
SGVP	5.1	yes	both	yes	yes	yes
RVP	5.2	yes	response	yes	yes	yes
LK	5.2.1	yes	response	no	yes	no
LVP	5.3.1	yes	latent	yes	no	yes
NNGPC	5.3.2	yes	latent	no	no	no

Table 2: Summary of the considered methods. Section: section in which the method is described; obs-pred: constraint that observed are ordered before prediction locations; obs cond: conditioning at observed locations; pred cond: prediction variables can condition on other prediction variables; linear: computational complexity guaranteed to be linear in  $n$ ; new: new method introduced in this paper



(a) Simulated data (dots), posterior means (solid lines) and pointwise 95% intervals (dashed lines)

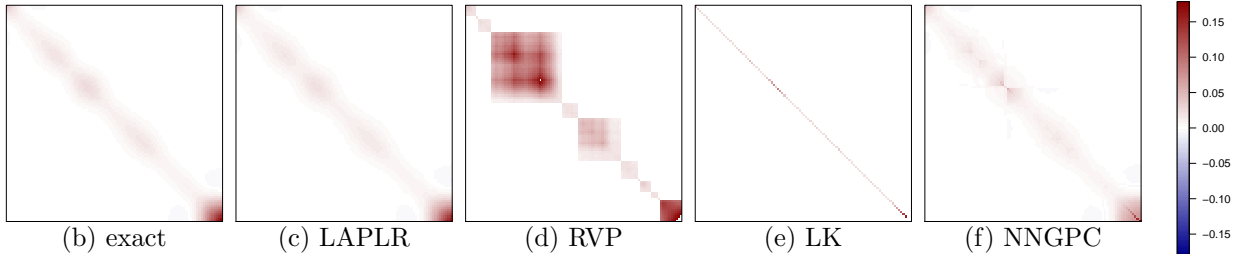


Figure 1: Illustration of predictions at  $n_P = 100$  locations based on  $n_O = 30$  simulated data on  $\mathbb{D} = [0, 1]$  for Matérn covariance with smoothness 1.5 using  $m = 2$  and coordinate (left-to-right) ordering. (b)–(f): Posterior predictive covariance matrices  $\Sigma_{pp}$



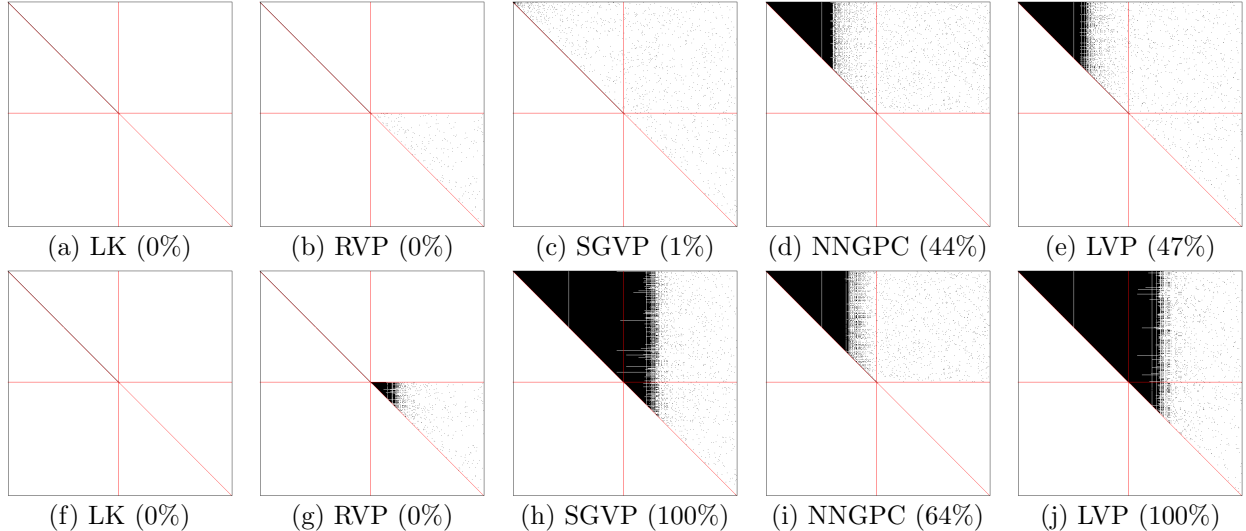


Figure 2: Sparsity structure of  $\mathbf{V} = \text{rchol}(\mathbf{W})$  for  $n_O = n_P = 1,000$  and  $m = 10$  on a unit square using maxmin ordering. Top row: matrices obtained using (6). Bottom row: obtained using “brute-force” Cholesky. Lines indicate the blocks from (6). Percentages indicate density (i.e., proportion of nonzero entries) in the upper triangle of  $\mathbf{V}_{oo}$ .

Computing  $\mathbf{V}$  using (6) is preferable to the “brute-force” Cholesky factorization  $\mathbf{V} = \text{rchol}(\mathbf{W})$  for two reasons. First, (6) avoids having to compute and factorize the entire matrix  $\mathbf{W}$ , because the last  $n_P$  columns of  $\mathbf{V}$  can simply be “copied” from  $\mathbf{A}$  (i.e.,  $\mathbf{V}_{\bullet p} = \mathbf{A}_{\bullet \bar{p}}$ ). The second (and more important) reason is that brute-force Cholesky factorization of  $\mathbf{W}$  can lead to a potentially very large number of “numerical nonzeros” in  $\mathbf{V}$ , which are symbolic nonzero entries in  $\mathbf{V}$  that are zero in theory but nonzero in practice due to numerical errors. These numerical nonzeros are illustrated in Figure 2, and described in detail in Appendix B.

## 5.1 Sparse general Vecchia prediction (SGVP)

Sparse general Vecchia prediction (SGVP) sets  $q_y(i) = q(i)$  for  $i \in p$ . For  $i \in o$ , SGVP follows the same rules as the SGV approach (Katzfuss and Guinness, 2017): Set  $q_y(i) \subset q(i)$  such that  $j < k$  can only both be in  $q_y(i)$  if  $j \in q_y(k)$ . The remaining conditioning indices are then assigned to  $q_z(i) = q(i) \setminus q_y(i)$ . This ensures sparsity of  $\mathbf{V}$ :

**PROPOSITION 2.** *Under SGVP conditioning, we have  $\mathbf{V}_{ji} = 0$  unless  $j = i$  or  $j \in q_y(i)$ . Hence,  $\mathbf{V}$  has at most  $m$  off-diagonal nonzero elements in each column.*

For all data examples, for SGVP we determine the set  $q_y(i)$  for  $i \in o$  similarly to the SGV in Katzfuss and Guinness (2017): For  $i = 1, \dots, n_O$ , define  $h(i) = \arg \max_{j \in q(i)} |q_y(j) \cap q(i)|$ ,  $k_i = \arg \min_{\ell \in h(i)} \|\mathbf{s}_i - \mathbf{s}_\ell\|$ , and then set  $q_y(i) = (k_i) \cup (q_y(k_i) \cap q(i))$ .

## 5.2 Response Vecchia prediction (RVP)

Response Vecchia prediction (RVP) is a special case of obs–pred ordering and of SGVP, in which the conditioning set for any  $y_i$  only includes elements of  $\mathbf{y}_p$  and the response vector  $\mathbf{z}_o$ , not of the latent  $\mathbf{y}_o$ ; that is, RVP sets  $q_y^o(i) = \emptyset$ .

From (7), we can see that this implies  $\mathbf{A}_{o\bar{p}} = \mathbf{0}$ , and so  $\mathbf{V} = \text{blockdiag}(\mathbf{V}_{oo}, \mathbf{A}_{p\bar{p}})$  and  $\mathbf{W} = \text{blockdiag}(\mathbf{W}_{oo}, \mathbf{W}_{pp})$  are both block-diagonal. (As a side note, it also implies that  $\mathbf{W}_{oo}$  and  $\mathbf{V}_{oo}$  are diagonal matrices.) Using our indexing notation,  $\mathbf{B}_{\bullet\bar{p}}$  refers to the last  $n_P$  columns of  $\mathbf{B}$  (i.e., those corresponding to  $\mathbf{y}_p$ ).

PROPOSITION 3. For RVP, we have  $\Sigma_{pp}^{-1} = \mathbf{W}_{pp} = \mathbf{A}_{p\bar{p}}\mathbf{A}'_{p\bar{p}}$ ,  $\boldsymbol{\mu}_p = (\mathbf{A}'_{p\bar{p}})^{-1}(\mathbf{B}_{\bullet\bar{p}})'\mathbf{z}$ , and  $\text{var}(\mathbf{H}_{p\bullet}\mathbf{y}_p|\mathbf{z}) = (\mathbf{A}_{p\bar{p}}^{-1}\mathbf{H}'_{p\bullet})'(\mathbf{A}_{p\bar{p}}^{-1}\mathbf{H}'_{p\bullet})$ .

Thus, when only prediction at unobserved locations  $\mathcal{S}_p$  is desired, the prediction tasks laid out in Section 3.4 can be carried out solely based on  $\mathbf{A}_{p\bar{p}}$  and  $\mathbf{B}_{\bullet\bar{p}}$ , which are both part of the last  $n_P$  columns of  $\mathbf{U}$  corresponding to  $\mathbf{y}_p$ . That is, the first  $2n_O$  columns of  $\mathbf{U}$  corresponding to  $\mathbf{y}_o$  and  $\mathbf{z}_o$  would then not be required for prediction, resulting in a prediction complexity that depends on  $n_P$ , not on  $n = n_O + n_P$ .

### 5.2.1 Local kriging (LK)

Local kriging (LK) is a special case of RVP obtained by setting  $q_y^p(i) = \emptyset$ ; that is, LK assumes that  $q_y(i) = \emptyset$  and  $q_z(i) = q(i) \subset o$  for all  $i = 1, \dots, n$ . To see that these assumptions result in local kriging, note that, from (7),  $\mathbf{A}_{pp}$  and hence  $\mathbf{W}_{pp}$  are now diagonal, and so using Proposition 3:

$$\begin{aligned} \Sigma_{pp} &= \mathbf{W}_{pp}^{-1} = \text{diag}(\{\mathbf{A}_{p_i\bar{p}_i}^2 : i = 1, \dots, n_P\})^{-1} = \text{diag}(\{r_i : i = n_O + 1, \dots, n_O + n_P\}) \\ &= \text{diag}(\{\text{var}(\mathbf{y}_{p_i}|\mathbf{z}_{q(i)}) : i = 1, \dots, n_P\}). \end{aligned}$$

Similarly, it is straightforward to show that  $\boldsymbol{\mu}_{p_i} = \text{E}(\mathbf{y}_{p_i}|\mathbf{z}_{q(i)})$ . The name local kriging comes from the fact that the prediction mean and variance depend only on the nearest  $m$  observations  $\mathbf{z}_{q(i)}$ .

Of course, the strong assumptions made for LK lead to fast, simple computations, but any posterior dependence between different elements of  $\mathbf{y}_p$  is completely ignored.

There is a strong connection to the nearest neighbor Gaussian process – response (NNGPR) of Finley et al. (2017). The likelihood in NNGPR is what we refer to here as standard or response Vecchia. Predictions for NNGPR are equivalent to LK, except that we here predict  $\mathbf{y}_p$  instead of predicting  $\mathbf{z}_p$  as in the NNGPR. The latter can be easily achieved by adding the noise or nugget variance to each prediction variance (see end of Section 2).

## 5.3 Latent Vecchia approaches

We now discuss two approaches that rely on completely latent conditioning, meaning that they assume  $q_z(i) = \emptyset$  for all  $i = 1, \dots, n$ . The problem with these approaches is that linear complexity cannot be guaranteed; see Figures 2 and 5 for illustration. Hence, we do not recommend these methods, but include them here solely for the purpose of comparison.

### 5.3.1 Latent Vecchia prediction (LVP)

Latent Vecchia prediction is a special case of obs–pred ordering with no additional restrictions, other than that conditioning must be completely latent; that is,  $q_z(i) = \emptyset$  and  $q_y(i) = q(i)$  for all  $i = 1, \dots, n$ .

### 5.3.2 Nearest-neighbor Gaussian process – collapsed (NNGPC)

Finley et al. (2017) consider an approach called NNGPC based on the NNGP in Datta et al. (2016). NNGPC can be viewed as a special case of general Vecchia using obs–pred ordering and assuming that  $\mathbf{y}_p$  is conditionally independent given  $\mathbf{y}_o$ ; that is, NNGPC is a special case of LVP with  $q_y^p(i) = \emptyset$ .

## 6 Summary and properties of the methods

All considered methods are summarized in Table 2. The first three methods are our new proposed approaches. LK and NNGPC are existing approaches. In the case of zero noise or nugget (i.e.,  $\tau_i = 0$  for all  $i = 1, \dots, n$ ), we have  $\mathbf{y} = \mathbf{z}$ , and so “obs cond” is not a distinguishing factor any more, and several of the methods become equivalent. Specifically, then LVP and SGVP become equivalent to RVP, while NNGPC becomes equivalent to LK.

### 6.1 Approximation accuracy

For a true distribution  $f$  implied by a GP model as in Section 2, let  $\hat{f}_{\text{SGVP}}$ ,  $\hat{f}_{\text{RVP}}$ ,  $\hat{f}_{\text{LK}}$ ,  $\hat{f}_{\text{NNGPC}}$ , and  $\hat{f}_{\text{LVP}}$  denote the approximate distributions implied by SGVP, RVP, LK, NNGPC, and LVP, respectively.

**PROPOSITION 4.** *Assume that the ordering of the locations  $\mathcal{S}$  and the conditioning indices  $q(i)$ ,  $i = 1, \dots, n$ , are fixed. Then, the following ordering of Kullback-Leibler (KL) divergences holds:*

$$\text{KL}(f(\mathbf{x})\|\hat{f}_{\text{LVP}}(\mathbf{x})) \leq \text{KL}(f(\mathbf{x})\|\hat{f}_{\text{SGVP}}(\mathbf{x})) \leq \text{KL}(f(\mathbf{x})\|\hat{f}_{\text{RVP}}(\mathbf{x})).$$

We also have

$$\text{KL}(f(\mathbf{x})\|\hat{f}_{\text{NNGPC}}(\mathbf{x})) \leq \text{KL}(f(\mathbf{x})\|\hat{f}_{\text{LK}}(\mathbf{x}))$$

if these two methods use the same ordering and same  $q(i)$ ,  $i = 1, \dots, n$ .

Thus, for a fixed ordering scheme (e.g., maxmin) and a fixed conditioning scheme (e.g., nearest-neighbor), the LVP approximation of the joint distribution of  $\mathbf{x} = \mathbf{y} \cup \mathbf{z}_o$  is as or more accurate as SGVP, which in turn is as or more accurate as RVP. The same holds for NNGPC versus LK. However, note that lower KL divergence for  $f(\mathbf{x})$  does not necessarily imply lower KL divergence for  $f(\mathbf{y}|\mathbf{z}_o) = f(\mathbf{x})/\int f(\mathbf{x})d\mathbf{y}$  or  $f(\mathbf{y}_p|\mathbf{z}_o)$  — see Section 7 for numerical examples.

In general, Vecchia approximations become more accurate as the conditioning-set size  $m$  increases (Guinness, 2018, Thm. 1). Indeed, we have  $\hat{f}(\mathbf{x}) \rightarrow f(\mathbf{x})$  and hence  $\hat{f}(\mathbf{y}|\mathbf{z}_o) \rightarrow f(\mathbf{y}|\mathbf{z}_o)$  as  $m \rightarrow n$  for most methods. However, for LK and NNGPC, due to the assumption of conditional independence of the entries in  $\mathbf{y}_p$  given  $\mathbf{z}_o$  and  $\mathbf{y}_o$  (in Table 2: pred cond = no), this convergence holds only marginally, in the sense that  $\hat{f}(\mathbf{y}_i|\mathbf{z}_o) \rightarrow f(\mathbf{y}_i|\mathbf{z}_o)$  but  $\hat{f}(\mathbf{y}|\mathbf{z}_o) \not\rightarrow f(\mathbf{y}|\mathbf{z}_o)$ . This is also shown numerically in Figures 3 and 4, Panels (a) and (b).

## 6.2 Computational complexity

As laid out in Section 3.4, the relevant quantities for prediction can be obtained by computing  $\mathbf{U}$ , calculating  $\mathbf{V}$  from  $\mathbf{U}$ , carrying out a selected inversion based on  $\mathbf{V}$ , and performing triangular solves in  $\mathbf{V}$ . The cost of computing  $\mathbf{U}$  is  $\mathcal{O}(nm^3)$ , the cost for each triangular solve in  $\mathbf{V}$  is on the order of the number of nonzeros in  $\mathbf{V}$ , and the cost of computing  $\mathbf{V}$  and the selected inversion is proportional to the sum of squares of the number of nonzeros per column in  $\mathbf{V}$ .

For LAPLR (see Section 4), and SGVP (see Proposition 2) and its special cases RVP and LK, the number of off-diagonal nonzeros in each column of  $\mathbf{V}$  is guaranteed to be at most  $m$ . For these methods,  $\mathbf{V}$  and the selected inverse can hence be computed in  $\mathcal{O}(nm^2)$  time,  $\mathbf{V}^{-1}\mathbf{H}'$  in  $\mathcal{O}(nm\ell)$  time, and  $(\mathbf{V}^{-1}\mathbf{H}')'(\mathbf{V}^{-1}\mathbf{H}')$  can be computed in  $\mathcal{O}(n\ell^2)$  time. (An additional approximation can be necessary for selected inversion in the case of obs-pred methods — see Appendix B.1 for details.)

Thus, the complexity of GP prediction using SGVP, RVP, and LK is linear in  $n$ . In contrast, LVP and NNGPC require purely latent conditioning (i.e., obs cond = latent in Table 2), and hence do not exhibit linear complexity. In that case, the matrix  $\mathbf{V}$  is often quite dense (see Figure 2), which can lead to long computation times (see Figure 5).

## 7 Simulation study

For numerical comparison of the methods in Table 2, we simulated 100 datasets by drawing locations  $\mathcal{S}_o$  from an independent uniform distribution on  $\mathbb{D}$ , and then sampling corresponding data  $\mathbf{z}$  from the true distribution  $f(\mathbf{z})$ , by simulating  $\mathbf{y}$  based on a Matérn covariance function with variance 1 and smoothness parameter  $\nu$ , plus noise with constant variance  $\tau^2$ . We call  $1/\tau^2$  the signal-to-noise ratio (SNR). For each dataset, we made predictions at an equidistant grid  $\mathcal{S}_p$  on  $\mathbb{D}$  using the considered methods.

We computed the KL divergence for the joint prediction distribution  $\hat{f}(\mathbf{y}_p|\mathbf{z}_o)$ , and averaged over the results for each method. This approximates the KL divergence with respect to the joint distribution of the observation locations  $\mathcal{S}_o$  and the observations  $\mathbf{z}_o$ . We also computed the average marginal KL divergence at the prediction locations:  $\hat{f}(\mathbf{y}_{p_i}|\mathbf{z}_o)$ ,  $i = 1, \dots, n_P$ . Finally, we computed root mean square errors (RMSEs). To be able to compute the KL divergence quickly for this large number of repetitions and settings, we used  $n_O = n_P = 100$ . A larger example can be found in Section 8.

### 7.1 Numerical comparison in 1-D

First, we considered the unit interval  $\mathbb{D} = [0, 1]$  and range parameter 0.1. All methods used coordinate (left-to-right) ordering. Our proposed method is LAPLR.

As shown in Figure 3, LAPLR is exact for  $\nu = 0.5$  with any  $m \geq 1$ . For  $\nu = 1.5$ , the method was still much more accurate than any of the other approaches. LK and NNGPC, which do not condition on prediction locations (pred cond = no in Table 2), could only achieve a certain level of accuracy, with the joint KL divergence leveling off as  $m$  increased. LK and NNGPC performed better in terms of marginal accuracy, as all of the methods

converged to zero marginal KL divergence as  $m$  increases. Likewise for RMSE, all of the methods converged to the optimal RMSE (which depends on the SNR) as  $m$  increased, with the methods that condition on latent variables (LAPLR, NNGPC, LVP) converging more quickly. In general, the larger the nugget or smoothness, the better the relative performance of methods that rely on latent conditioning.

## 7.2 Numerical comparison in 2-D

On the unit square,  $\mathbb{D} = [0, 1]^2$ , we used a range parameter of 0.8. All methods used maxmin ordering. As can be seen in Figure 4, LVP performed best, but as we will see in Section 7.3, it is not computationally scalable. Out of the other approaches, SGVP performed well in terms of both joint and marginal accuracy measures. The joint KL divergence did not converge to zero for approaches that use independent conditioning for the prediction locations (LK and NNGPC). NNGPC was competitive with the other methods on marginal measures, as expected. The larger the nugget or smoothness, the better the relative performance of methods that rely on latent conditioning (SGVP, NNGPC, and LVP).

## 7.3 Timing comparison

We also carried out a timing study that examined the time for computing  $\mathbf{U}$  and  $\mathbf{V}_{oo}$  as a function of  $n_O$  on a unit square. (As shown in (6), only the submatrix  $\mathbf{V}_{oo}$  of  $\mathbf{V}$  has to be computed, while the remaining parts of  $\mathbf{V}$  can simply be copied from  $\mathbf{U}$ .) Median computation times from five repetitions are shown in Figure 5. Consistent with our theoretical results, the time for computing  $\mathbf{U}$  increased roughly linearly with  $n$ , and was the same for all methods for given  $n$  and  $m$ . For SGVP, RVP, and LK, the time for computing  $\mathbf{V}$  was negligible relative to that for computing  $\mathbf{U}$ . For NNGPC and LVP, the time for computing  $\mathbf{V}$  increased quickly, and it was already an order of magnitude larger than that for computing  $\mathbf{U}$  with relatively moderate data sizes  $n_O$  in the tens of thousands. Note that we computed the Cholesky factor  $\mathbf{V}_{oo} = \text{rchol}(\mathbf{A}_{o\bar{o}}\mathbf{A}'_{o\bar{o}})$  under reverse ordering for all methods. Commonly used heuristic ordering methods for obtaining sparse Cholesky factors might improve computation times for NNGPC and LVP, although this would generally not allow usage of the block form in (6), and hence the Cholesky algorithm would need to be applied to the entire  $\mathbf{W}$  matrix.

# 8 Application to satellite data

We applied some of the discussed methods to Level-2 bias-corrected solar-induced chlorophyll fluorescence retrievals over land from the Orbiting Carbon Observatory 2 (OCO-2) satellite (OCO-2 Science Team et al., 2015). The OCO-2 satellite has a sun-synchronous orbit with a period of 99 minutes and repeats its spatial coverage every 16 days. We analyzed chlorophyll fluorescence data collected during one repeat cycle from May 16 to May 31, 2017 over the contiguous United States. During this time period, there are a total of 104,683 observations, plotted in Figure 6a. There was little evidence of temporal change during the time period, so we restricted our attention to a purely spatial model.

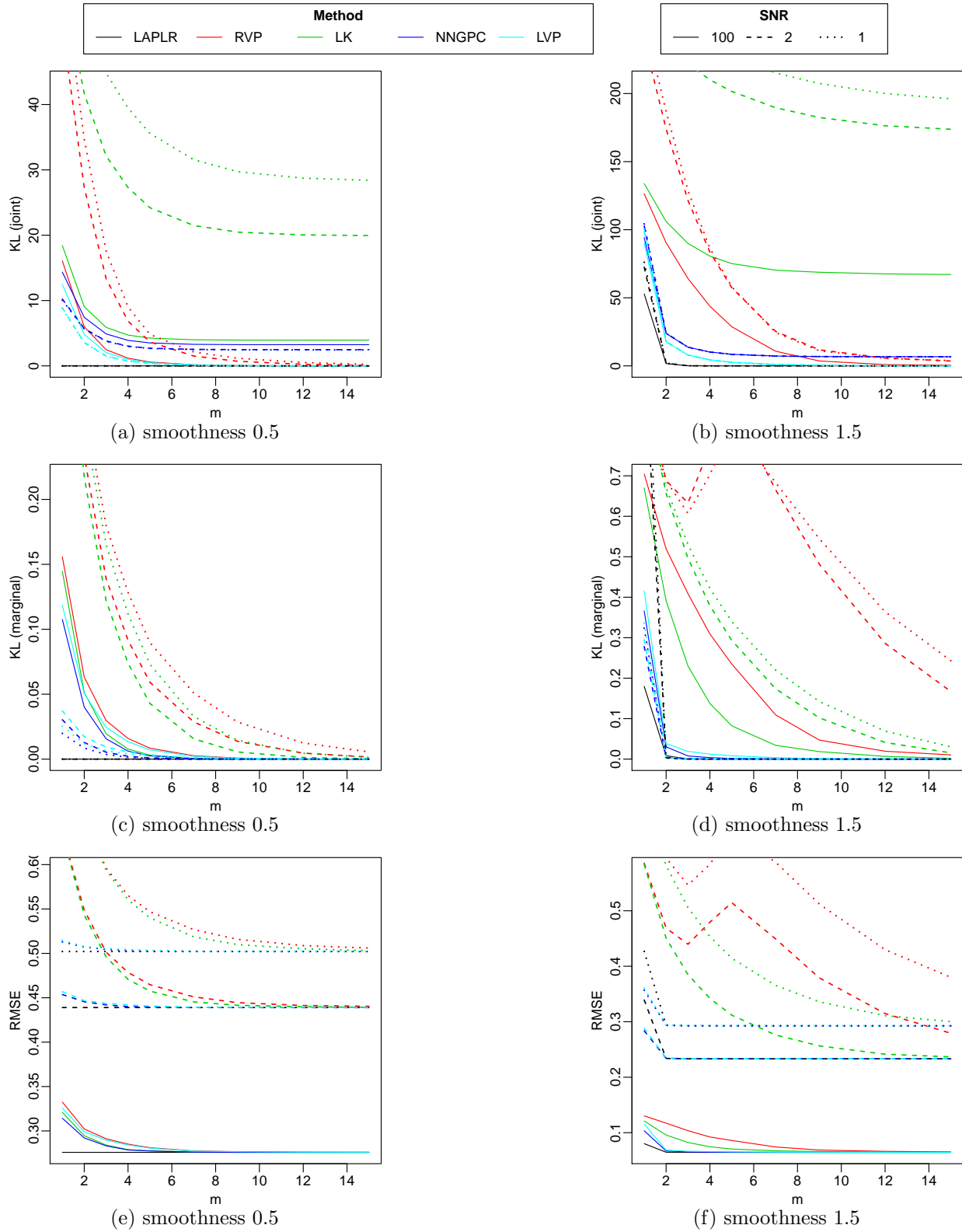


Figure 3: Accuracy scores for posterior predictive distributions in 1-D

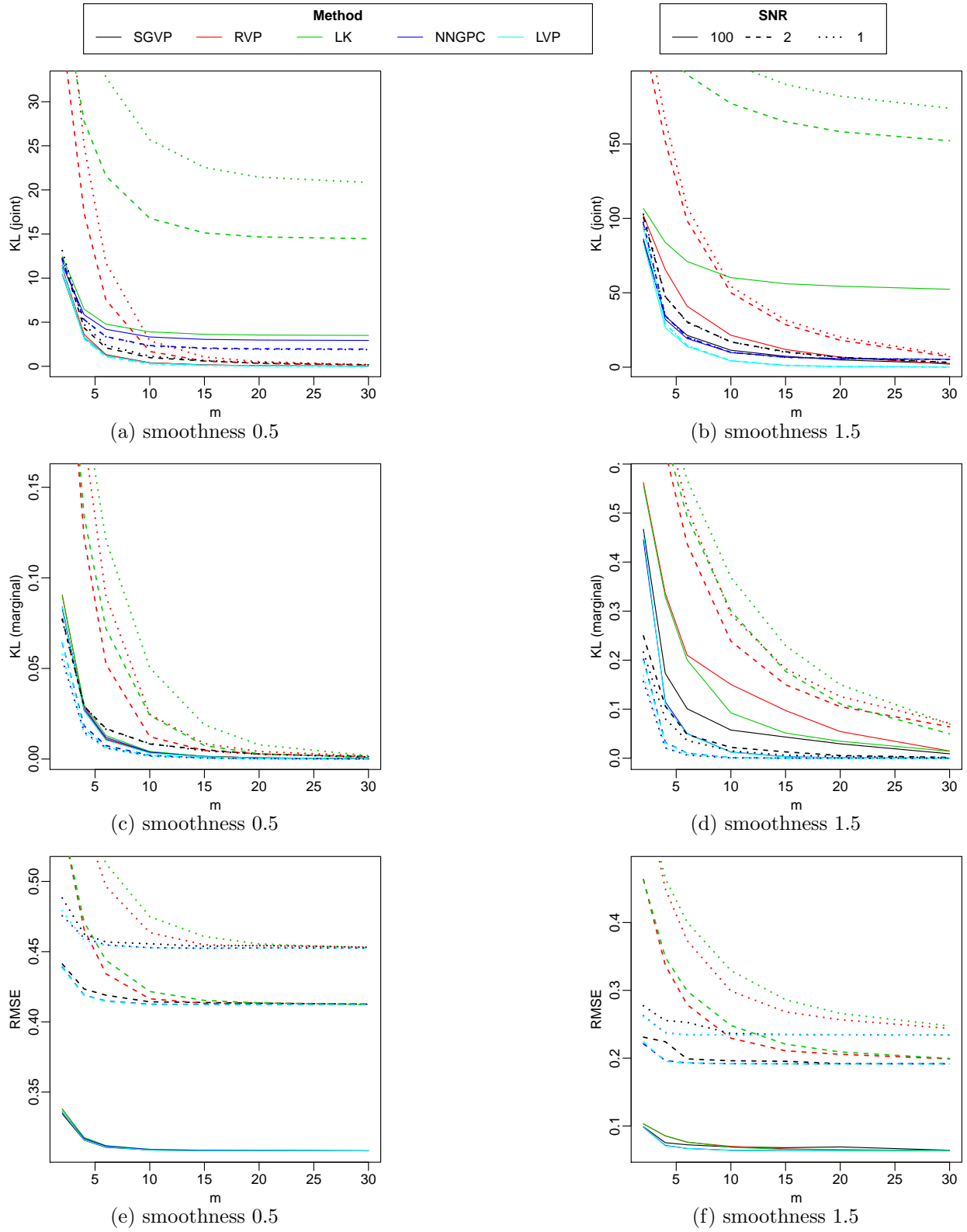


Figure 4: Accuracy scores for posterior predictive distributions in 2-D

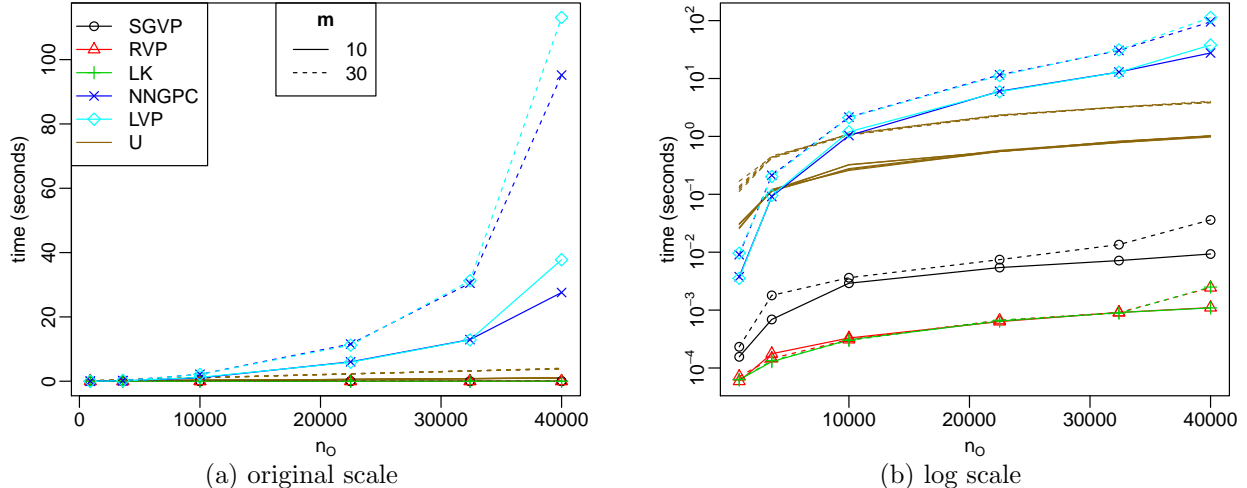


Figure 5: Time for computing  $\mathbf{U}$  and  $\mathbf{V}_{oo}$  for  $n_O = n_P$  observed and prediction locations on a unit square, as a function of  $n_O$ . Time for computing  $\mathbf{U}$  does not depend on the method. Time for computing  $\mathbf{V}_{oo}$  is close to zero for SGVP, RVP, and LK.

After subtracting a constant mean, we assumed that the data  $\mathbf{z}$  were noisy observations of a true chlorophyll fluorescence field  $y(\cdot) \sim GP(0, K)$ , where  $K$  was assumed to be an isotropic covariance function given by the sum of an exponential and squared exponential covariance:

$$K(\mathbf{s}_i, \mathbf{s}_j) = \sigma_e^2 \exp(-\|\mathbf{s}_1 - \mathbf{s}_2\|/\alpha_e) + \sigma_s^2 \exp(-\|\mathbf{s}_1 - \mathbf{s}_2\|^2/\alpha_s^2), \quad \mathbf{s}_i, \mathbf{s}_j \in \mathbb{D},$$

where the squared exponential term was added to enable long-range predictions. The noise was assumed to have constant variance  $\tau^2$ .

First, we estimated the covariance parameters based on the entire dataset using the SGV method, increasing  $m$  up to 40 for convergence to the exact GP. As the likelihood was not informative regarding  $\sigma_s$  and  $\alpha_s$ , we estimated these parameters based on the log score achieved for held-out swaths using cross-validation. We then estimated the remaining parameters,  $\sigma_e$ ,  $\alpha_e$ , and  $\tau$  based on the likelihood. This procedure roughly resulted in the estimates  $\hat{\sigma}_e = 0.7$ ,  $\hat{\alpha}_e = 2.12\text{km}$ ,  $\hat{\sigma}_s = 0.53$ ,  $\hat{\alpha}_s = 4247\text{km}$ , and  $\hat{\tau} = 0.62$ .

Then, using the obtained covariance function and noise variance, we computed predictions for the scalable methods SGVP, RVP, and LK at a grid of size  $n_P = 22,500$ . Figure 6 shows predictions for  $m = 20$ . The predictions using SGVP look most natural, while the RVP plot looks slightly noisier, and the LK plot exhibits undesirable streaks in the East-West direction.

We also compared the prediction accuracy of SGVP, RVP, and LK via two cross-validation experiments. First, we carried out 20-fold cross-validation, with each fold selecting 5% of the data as test data completely at random, to evaluate short-range prediction. Second, we held out each of the 34 swaths, one at a time, to evaluate long-range prediction. For each of the two cross-validation experiments, we computed the root mean squared error (RMSE) and the total log score, obtained by summing the negative log likelihoods for each held out test set. The log score is a proper scoring rule that evaluates the approximation error in the joint predictive distribution (e.g., Gneiting and Katzfuss, 2014). Note that we did not know



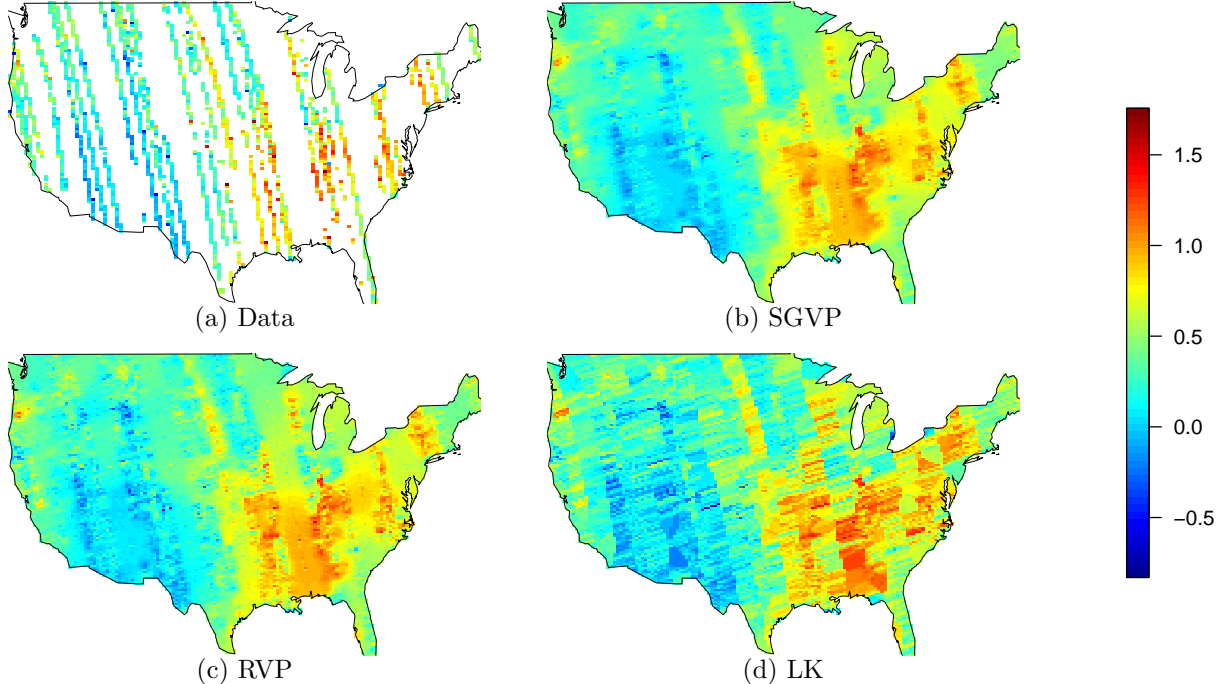


Figure 6: Satellite data, together with Vecchia predictions using  $m = 20$

the true fluorescence values  $\mathbf{y}_p$ , and so all comparisons were carried out relative to the (very noisy) test data  $\mathbf{z}_p$ .

The resulting prediction scores are shown in Figure 7. For all settings, SGVP achieved lower (i.e., better) scores than RVP, which in turn performed better than LK. The log scores of our new methods SGVP and RVP were fairly similar, while the log score of LK was considerably worse, as expected. RVP roughly required  $m = 40$  to achieve the same RMSPE as SGVP with  $m = 20$ , while LK required roughly two-to-four times the  $m$  of SGVP to achieve the same RMSPE. These differences can be substantial in terms of computation times, which scale cubically in  $m$ .

## 9 Conclusions

Vecchia approximations of Gaussian processes (GPs) are a powerful computational tool for enabling fast analysis of large spatial datasets. While Vecchia approximations have been very popular for likelihood approximations, their use for the very important task of GP prediction or kriging had not been fully examined. Here, we proposed a general Vecchia framework for GP predictions, which includes as special cases some existing and several novel computational approaches. We studied the accuracy and computational properties of the methods both theoretically and numerically.

Based on our results, we make the following recommendations. On a one-dimensional domain, LAPLR clearly had the best performance in all of the settings we considered. The auto-regressive structure in LAPLR also affords linear computational scaling, and so we recommend LAPLR without any qualifications when the domain is one-dimensional. In two

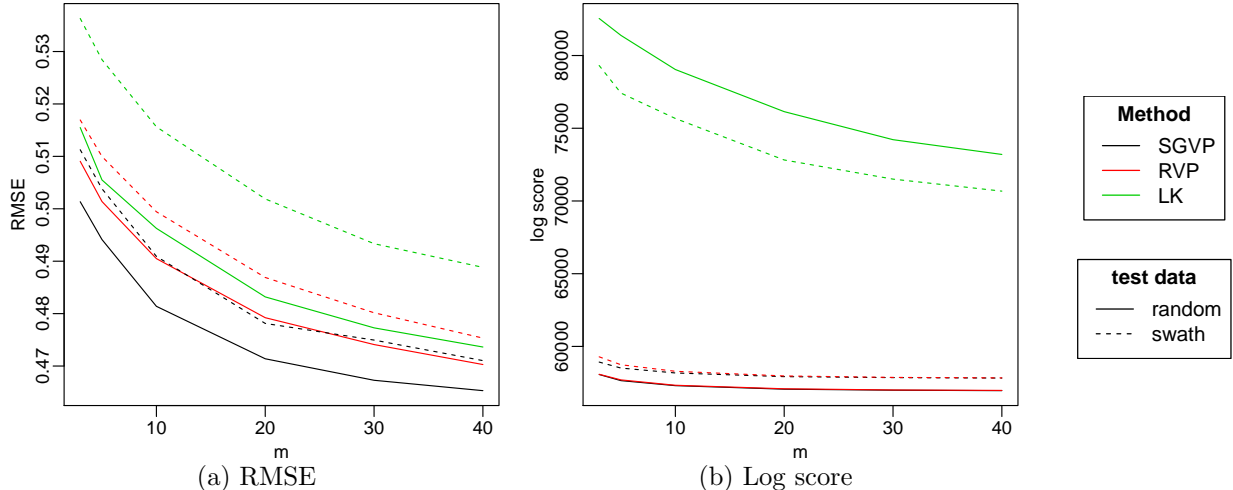


Figure 7: Comparison of prediction accuracy for the fluorescence data

dimensions, there are clear advantages to conditioning on latent variables when the signal-to-noise ratio is low. SGVP achieves linear scaling and conditions on some latent variables, and so, based on its performance in the numerical examples, we recommend using SGVP for the low signal-to-noise case. RVP has some computational advantages over SGVP and performed well in the high signal-to-noise case, and so we recommend RVP in two dimensions when the nugget is small or zero. RVP converges to the true predictive distribution as  $m$  increases, but this convergence was slower than that of SGVP, especially in the presence of noise. Local kriging (LK), or NNGP–response, is fast and can provide accurate marginal predictive distributions, but it is not capable of characterizing joint predictive distributions. LVP can be very accurate but does not scale linearly and so is computationally burdensome. NNGPC does not scale linearly and is not capable of characterizing joint predictive distributions.

The methods and algorithms proposed here are implemented in the R package `GPvecchia` available at <https://github.com/katzfuss-group/GPvecchia>. The default settings of the package functions reflect the recommendations in the previous paragraph. In principle, our methods and the code are applicable in more than two dimensions, but a thorough investigation of their properties in this context will be carried out in future work.

## Acknowledgments

Katzfuss’ research was partially supported by National Science Foundation (NSF) grant DMS–1521676 and NSF CAREER grant DMS–1654083. Guinness’ research was partially supported by NSF grant DMS–1613219 and NIH grant No. R01ES027892. Daniel Zilber contributed to the R package `GPvecchia`.

## A Computing U

To obtain  $\mathbf{U}$ , let  $g(i)$  denote the vector of indices of the elements in  $\mathbf{x}$  on which  $x_i$  conditions. More precisely, for  $x_i = z_k$  we have  $g(i) = (i-1)$ , because  $z_k$  only conditions on the variable  $y_k$ , which is ordered immediately prior to  $z_k$  in  $\mathbf{x}$ . For  $x_i = y_k$ ,  $g(i)$  represents the indices of the variables in  $\mathbf{y}_{q_y(k)}$  and  $\mathbf{z}_{q_z(k)}$  in  $\mathbf{x}$ , so that  $\mathbf{x}_{g(i)}$  consists of the elements of  $\mathbf{y}_{q_y(k)}$  and  $\mathbf{z}_{q_z(k)}$ . Also define  $C(x_i, x_j)$  as the covariance between  $x_i$  and  $x_j$  implied by the true model in Section 2; that is,  $C(y_i, y_j) = C(z_i, y_j) = K(\mathbf{s}_i, \mathbf{s}_j)$  and  $C(z_i, z_j) = K(\mathbf{s}_i, \mathbf{s}_j) + \mathbb{1}_{i=j}\tau_i^2$ .

Then, the  $(j, i)$ th element of  $\mathbf{U}$  can be calculated as

$$\mathbf{U}_{ji} = \begin{cases} r_i^{-1/2}, & i = j, \\ -b_i^{(j)} r_i^{-1/2}, & j \in g(i), \\ 0, & \text{otherwise,} \end{cases} \quad (7)$$

where  $\mathbf{b}'_i = C(x_i, \mathbf{x}_{g(i)})C(\mathbf{x}_{g(i)}, \mathbf{x}_{g(i)})^{-1}$ ,  $r_i = C(x_i, x_i) - \mathbf{b}'_i C(\mathbf{x}_{g(i)}, x_i)$ , and  $b_i^{(j)}$  denotes the  $k$ th element of  $\mathbf{b}_i$  if  $j$  is the  $k$ th element in  $g(i)$  (i.e.,  $b_i^{(j)}$  is the element of  $\mathbf{b}_i$  corresponding to  $x_j$ ). For example, if  $x_i = z_k$ , it is straightforward to show that  $\mathbf{b}_i = 1$  and  $r_i = \tau_k^2$ , and so the  $i$ th column of  $\mathbf{U}$  is all zero except for  $\mathbf{U}_{i,i} = 1/\tau_k$  and  $\mathbf{U}_{i-1,i} = -1/\tau_k$ .

## B Numerical nonzeros in $\mathbf{V}$ under obs–pred ordering

For simplicity, we focus here on the case of SGVP described in Section 5.1, although numerical nonzeros can also arise for the other obs–pred methods (see Figure 2). For SGVP, the upper triangle of  $\mathbf{W}$  is at least as dense as the upper triangle of  $\mathbf{V}$ :

PROPOSITION 5. *For SGVP and  $j < i$ , we have  $\mathbf{V}_{ji} = 0$  if  $\mathbf{W}_{ji} = 0$ .*

Thus, there may be pairs  $j < i$  such that  $\mathbf{V}_{ji} = 0$  but  $\mathbf{W}_{ji} \neq 0$ . From the standard Cholesky algorithm, we can derive that the algorithm for  $\mathbf{V} = \text{rchol}(\mathbf{W})$  computes  $\mathbf{V}_{ji}$  as

$$\mathbf{V}_{ji} = (\mathbf{W}_{ji} - \sum_{k=i+1}^n \mathbf{V}_{ik} \mathbf{V}_{jk}) / \mathbf{V}_{ii}.$$

Consider the difference in the parentheses for a pair  $j < i$  such that  $\mathbf{V}_{ji} = 0$  but  $\mathbf{W}_{ji} \neq 0$ . We then know that the difference is zero, and so  $\mathbf{W}_{ji} = \sum_{k=i+1}^n \mathbf{V}_{ik} \mathbf{V}_{jk}$ . However, it is not guaranteed that these two terms will indeed be exactly equal numerically, in that rounding error can occur in  $\sum_{k=i+1}^n \mathbf{V}_{ik} \mathbf{V}_{jk}$ , which relies on (potentially many) previous calculations in the Cholesky algorithm. Whenever such numerical error occurs, a numerical nonzero is introduced in  $\mathbf{V}$ .

Calculating  $\mathbf{V}$  using the block-matrix expression in (6) avoids such numerical nonzeros. This is easy to see for the last  $n_P$  columns in  $\mathbf{V}$ , which are simply copied from  $\mathbf{A}$  (and hence from  $\mathbf{U}$ ). The remaining block in  $\mathbf{V}$  is calculated as  $\mathbf{V}_{oo} = \text{rchol}(\mathbf{F})$ , where  $\mathbf{F} = \mathbf{A}_{o\bar{o}} \mathbf{A}'_{o\bar{o}}$  is equivalent to the matrix  $\mathbf{W}$  in Katzfuss and Guinness (2017) obtained solely based on  $\mathbf{x}_{\bar{o}}$  (i.e., ignoring  $\mathbf{y}_p$ ). Thus, from Katzfuss and Guinness (2017, Prop. 3.2), we see that for  $j < i$ ,  $\mathbf{F}_{ji} = 0$  unless  $j \in q_y(i)$ . From Proposition 2, we have  $\mathbf{V}_{ji} = 0$  unless  $j \in q_y(i)$ . Thus, for  $j < i$ ,  $\mathbf{F}_{ji} \neq 0$  if and only if  $\mathbf{V}_{ji} \neq 0$ , and so no numerical cancellations need to occur and no numerical nonzeros are introduced when computing  $\mathbf{V}$  using the block-matrix expression in (6).

### B.1 Implications for selected inverse

Under obs–pred ordering,  $\mathbf{V}$  is computed using the block-matrix expression in (6) to avoid numerical nonzeros. Because the submatrix  $\mathbf{V}_{oo}$  is calculated using the Cholesky algorithm, the posterior variances of  $\mathbf{y}_o$  at the observed locations can be computed exactly using  $\text{SelInv}(\mathbf{V}_{oo})$ . However, the selected inverse of  $\mathbf{V}$  is not guaranteed to return the exact posterior variances of  $\mathbf{y}_p$  at prediction locations, unless  $\mathbf{V}$  is “padded” with zeros, but then the selected inverse cannot be carried out in linear time even under SGVP rules.

This is because the selected inverse operates on the symbolic nonzero elements; that is, it operates on all elements that have to be computed in the Cholesky, even if they cancel to zero numerically (which is the case for many entries in our case). Denoting by  $\mathbf{S}$  the selected inverse of  $\mathbf{W}$  based on  $\mathbf{V}$ , a close look at the Takahashi recursions reveals that for all  $j, k$  with  $j, k \in q_y(i)$ , we need  $\mathbf{S}_{ji}$  and  $\mathbf{S}_{kj}$ . For SGVP with  $i \in p$ , the latter element is only calculated if  $j \in q_y(k)$ . However, if  $j \notin q_y(k)$ ,  $\mathbf{S}_{kj} = \text{cov}(y_j, y_k | \mathbf{z})$  will typically be very small (if  $m$  is reasonably large), because their corresponding locations will likely be far away from each other and data can be observed in between. In our experiments, the additional approximation error introduced by the selected inverse was negligible relative to the error introduced by the Vecchia approximation itself. When  $m$  becomes large enough for the Vecchia approximation to be accurate, the additional approximation error introduced by SelInv goes to zero as well.

If exact variances at prediction locations are required (i.e., no *additional* error is to be introduced by the selected inversion), they can be computed as  $\text{diag}(\text{var}(\mathbf{y}_p|\mathbf{z}_o)) = ((\mathbf{V}^{-1}\mathbf{I}_{\bullet p}) \circ (\mathbf{V}^{-1}\mathbf{I}_{\bullet p}))'\mathbf{1}_n$ . For SGVP and its special cases, this requires  $\mathcal{O}(nmn_P)$  time, as described in Section 6.2, and so the overall computational complexity would not be increased if  $n_P = \mathcal{O}(m^2)$ .

## C Proofs

In this section, we provide proofs for the propositions stated throughout the article.

*Proof of Proposition 1.* Partition  $\mathbf{W}$  similarly to  $\mathbf{V}$ :

$$\mathbf{W} = \begin{pmatrix} \mathbf{W}_{oo} & \mathbf{W}_{op} \\ \mathbf{W}_{po} & \mathbf{W}_{pp} \end{pmatrix}.$$

Because  $\mathbf{W} = \mathbf{A}\mathbf{A}'$ , where  $\mathbf{A}$  can be partitioned as in (5), we have

$$\begin{aligned} \mathbf{W}_{oo} &= \mathbf{A}_{o\bar{o}}\mathbf{A}'_{o\bar{o}} + \mathbf{A}_{o\bar{p}}\mathbf{A}'_{o\bar{p}}, \\ \mathbf{W}_{op} &= \mathbf{W}'_{po} = \mathbf{A}_{o\bar{o}}\mathbf{0}' + \mathbf{A}_{o\bar{p}}\mathbf{A}'_{p\bar{p}} = \mathbf{A}_{o\bar{p}}\mathbf{A}'_{p\bar{p}}, \\ \mathbf{W}_{pp} &= \mathbf{0}\mathbf{0}' + \mathbf{A}_{p\bar{p}}\mathbf{A}'_{p\bar{p}} = \mathbf{A}_{p\bar{p}}\mathbf{A}'_{p\bar{p}}. \end{aligned}$$

This implies that  $\mathbf{A}_{p\bar{p}} = \text{rchol}(\mathbf{W}_{pp})$ , because  $\mathbf{A}_{p\bar{p}}$  is upper triangular with positive entries on the diagonal.

Consider a generic block matrix  $\mathbf{M}$ , with

$$\mathbf{M} = \begin{pmatrix} \mathbf{M}_{11} & \mathbf{M}_{12} \\ \mathbf{M}_{21} & \mathbf{M}_{22} \end{pmatrix}, \quad \text{and so} \quad \text{rev}(\mathbf{M}) = \begin{pmatrix} \text{rev}(\mathbf{M}_{22}) & \text{rev}(\mathbf{M}_{21}) \\ \text{rev}(\mathbf{M}_{12}) & \text{rev}(\mathbf{M}_{11}) \end{pmatrix}.$$

Applying the well-known formula for the (lower triangular) Cholesky factor of a block-matrix, and then reverse-ordering the result, we obtain

$$\text{rchol}(\mathbf{M}) = \text{rev}(\text{chol}(\text{rev}(\mathbf{M}))) = \begin{pmatrix} \text{rchol}(\mathbf{S}) & \mathbf{M}_{12}(\text{rchol}(\mathbf{M}_{22})')^{-1} \\ \mathbf{0} & \text{rchol}(\mathbf{M}_{22}) \end{pmatrix},$$

where  $\mathbf{S} = \mathbf{M}_{11} - \mathbf{M}_{12}\mathbf{M}_{22}^{-1}\mathbf{M}_{21}$ .

Applying this result for the reverse Cholesky factor of a block matrix to  $\mathbf{W}$ , we obtain

$$\mathbf{V} = \text{rchol}(\mathbf{W}) = \begin{pmatrix} \mathbf{V}_{oo} & \mathbf{V}_{op} \\ \mathbf{0} & \mathbf{V}_{pp} \end{pmatrix},$$

where

$$\begin{aligned} \mathbf{V}_{pp} &= \text{rchol}(\mathbf{W}_{pp}) = \mathbf{A}_{p\bar{p}}, \\ \mathbf{V}_{op} &= \mathbf{W}_{op}(\text{rchol}(\mathbf{W}_{pp})')^{-1} = \mathbf{A}_{o\bar{p}}\mathbf{A}'_{p\bar{p}}(\mathbf{A}'_{p\bar{p}})^{-1} = \mathbf{A}_{o\bar{p}}, \\ \mathbf{V}_{oo} &= \text{rchol}(\mathbf{F}), \end{aligned}$$

and

$$\begin{aligned} \mathbf{F} &= \mathbf{W}_{oo} - \mathbf{W}_{op}\mathbf{W}_{pp}^{-1}\mathbf{W}_{po} \\ &= \mathbf{A}_{o\bar{o}}\mathbf{A}'_{o\bar{o}} + \mathbf{A}_{o\bar{p}}\mathbf{A}'_{o\bar{p}} - \mathbf{A}_{o\bar{p}}\mathbf{A}'_{p\bar{p}}(\mathbf{A}_{p\bar{p}}\mathbf{A}'_{p\bar{p}})^{-1}\mathbf{A}_{p\bar{p}}\mathbf{A}'_{o\bar{p}} \\ &= \mathbf{A}_{o\bar{o}}\mathbf{A}'_{o\bar{o}}. \end{aligned}$$

□

*Proof of Proposition 2.* First, in the graph terminology used in Katzfuss and Guinness (2017), note that any  $y_k$  with  $k \in p$  cannot have observed descendants under obs–pred ordering. Thus, using Prop. 3.3 in Katzfuss and Guinness (2017), we simply follow the proof of Prop. 6 in Katzfuss and Guinness (2017), considering only the graph formed by  $\{y_i : i \in o\}$ , to show that  $\mathbf{V}_{ji} = 0$  unless  $j = i$  or  $j \in q_y(i)$ , for  $i \in o = (1, \dots, n_o)$ . It is easy to see from the expression (6) and the definition of  $\mathbf{U}$  in (7), that the same holds for the last  $n_p$  columns of  $\mathbf{V}$  (i.e., for  $i \in p$ ). This proves that  $\mathbf{V}_{ji} = 0$  unless  $j = i$  or  $j \in q_y(i)$ .

Further, we have  $q_y(i) \subset q(i)$ , and we have assumed that  $|q(i)| \leq m$ . Thus, for SGVP,  $\mathbf{V}$  has at most  $m$  off-diagonal nonzero entries in each column.  $\square$

*Proof of Proposition 3.* Everything is trivial to show, except the posterior mean. We have  $\boldsymbol{\mu} = (\boldsymbol{\mu}'_o, \boldsymbol{\mu}'_p)'$  with  $\boldsymbol{\mu} = -(\mathbf{V}')^{-1}\mathbf{V}^{-1}\mathbf{A}\mathbf{B}'\mathbf{z}$ . Because  $\mathbf{V}$  and  $\mathbf{A}$  are blockdiagonal, so is the matrix product  $(\mathbf{V}')^{-1}\mathbf{V}^{-1}\mathbf{A}$ , and so  $\boldsymbol{\mu}_p = (\mathbf{A}'_{pp})^{-1}\mathbf{A}^{-1}_{pp}\mathbf{A}_{pp}(\mathbf{B}_{\bullet p})'\mathbf{z} = (\mathbf{A}'_{pp})^{-1}(\mathbf{B}_{\bullet p})'\mathbf{z}$ .  $\square$

*Proof of Proposition 4.* Thm. 1 in Guinness (2018) says that adding variables to the conditioning vector in Vecchia approximations cannot increase the KL divergence from the true model. Further, according to Katzfuss and Guinness (2017, Prop. 4), in our general Vecchia setting, moving an index  $j$  from  $q_z(i)$  to  $q_y(i)$  is equivalent to adding  $y_j$  to the conditioning vector of  $y_i$ . We have  $q_y^{\text{RVP}}(i) \subset q_y^{\text{SGVP}}(i) \subset q_y^{\text{LVP}}(i)$  for all  $i = 1, \dots, n$ , because  $q_y^{\text{RVP}}(i) = \emptyset$  for  $i \in o$ ,  $q_y^{\text{SGVP}}(i) = q(i)$  for  $i \in p$ , and  $q_y^{\text{LVP}}(i) = q(i)$  for all  $i = 1, \dots, n$ , which proves the first part of the proposition. Similarly, for the second part, we have  $q_y^{\text{LK}}(i) \subset q_y^{\text{NNGPC}}(i)$ , because  $q_y^{\text{LK}}(i) = \emptyset$  and  $q_y^{\text{NNGPC}}(i) = q(i)$  for all  $i = 1, \dots, n$ .  $\square$

*Proof of Proposition 5.* Assume SGVP conditioning and  $j < i$  throughout this proof. From Proposition 2, we have that  $\mathbf{V}_{ji} = 0$  unless  $j \in q_y(i)$ . From Katzfuss and Guinness (2017, Prop. 3.2), we have that  $\mathbf{W}_{ji} = 0$  unless  $j \in q_y(i)$  or  $\exists k > i$  such that  $i, j \in q_y(k)$ . Note that the SGVP rules for determining each  $q_y(k)$  ensure that if  $i, j \in q_y(k)$  for  $k \in o$ , then we must also have  $j \in q_y(i)$ . However, there are no such restrictions for  $q_y(k)$  with  $k \in p$ . Thus, we have  $\mathbf{V}_{ji} = 0$  if  $\mathbf{W}_{ji} = 0$ . On the other hand, for any pair  $j < i$  such that  $j \notin q_y(i)$  but  $i, j \in q_y(k)$  for some  $k$  with  $i < k \leq n_o$ , we have  $\mathbf{V}_{ji} = 0$  and  $\mathbf{W}_{ji} \neq 0$ .  $\square$

## References

- Banerjee, S., Carlin, B. P., and Gelfand, A. E. (2004). *Hierarchical Modeling and Analysis for Spatial Data*. Chapman & Hall.
- Banerjee, S., Gelfand, A. E., Finley, A. O., and Sang, H. (2008). Gaussian predictive process models for large spatial data sets. *Journal of the Royal Statistical Society, Series B*, 70(4):825–848.
- Cressie, N. and Johannesson, G. (2008). Fixed rank kriging for very large spatial data sets. *Journal of the Royal Statistical Society, Series B*, 70(1):209–226.
- Cressie, N. and Wikle, C. K. (2011). *Statistics for Spatio-Temporal Data*. Wiley, Hoboken, NJ.
- Datta, A., Banerjee, S., Finley, A. O., and Gelfand, A. E. (2016). Hierarchical nearest-neighbor Gaussian process models for large geostatistical datasets. *Journal of the American Statistical Association*, 111(514):800–812.
- Du, J., Zhang, H., and Mandrekar, V. S. (2009). Fixed-domain asymptotic properties of tapered maximum likelihood estimators. *The Annals of Statistics*, 37:3330–3361.
- Erisman, A. M. and Tinney, W. F. (1975). On computing certain elements of the inverse of a sparse matrix. *Communications of the ACM*, 18(3):177–179.
- Finley, A. O., Datta, A., Cook, B. C., Morton, D. C., Andersen, H. E., and Banerjee, S. (2017). Efficient algorithms for Bayesian nearest neighbor Gaussian processes. *arXiv:1702.00434*.
- Finley, A. O., Sang, H., Banerjee, S., and Gelfand, A. E. (2009). Improving the performance of predictive process modeling for large datasets. *Computational Statistics & Data Analysis*, 53(8):2873–2884.
- Furrer, R., Genton, M. G., and Nychka, D. (2006). Covariance tapering for interpolation of large spatial datasets. *Journal of Computational and Graphical Statistics*, 15(3):502–523.
- Gneiting, T. and Katzfuss, M. (2014). Probabilistic forecasting. *Annual Review of Statistics and Its Application*, 1(1):125–151.

- Guinness, J. (2018). Permutation and grouping methods for sharpening Gaussian process approximations. *Technometrics*.
- Higdon, D. (1998). A process-convolution approach to modelling temperatures in the North Atlantic Ocean. *Environmental and Ecological Statistics*, 5(2):173–190.
- Katzfuss, M. (2017). A multi-resolution approximation for massive spatial datasets. *Journal of the American Statistical Association*, 112(517):201–214.
- Katzfuss, M. and Cressie, N. (2011). Spatio-temporal smoothing and EM estimation for massive remote-sensing data sets. *Journal of Time Series Analysis*, 32(4):430–446.
- Katzfuss, M. and Gong, W. (2017). Multi-resolution approximations of Gaussian processes for large spatial datasets. *arXiv:1710.08976*.
- Katzfuss, M. and Guinness, J. (2017). A general framework for Vecchia approximations of Gaussian processes. *arXiv:1708.06302*.
- Kaufman, C. G., Schervish, M. J., and Nychka, D. W. (2008). Covariance tapering for likelihood-based estimation in large spatial data sets. *Journal of the American Statistical Association*, 103(484):1545–1555.
- Kennedy, M. C. and O’Hagan, A. (2001). Bayesian calibration of computer models. *Journal of the Royal Statistical Society: Series B*, 63(3):425–464.
- Li, S., Ahmed, S., Klimeck, G., and Darve, E. (2008). Computing entries of the inverse of a sparse matrix using the FIND algorithm. *Journal of Computational Physics*, 227(22):9408–9427.
- Lin, L., Yang, C., Meza, J., Lu, J., Ying, L., and Weinan, E. (2011). SelInv - An algorithm for selected inversion of a sparse symmetric matrix. *ACM Transactions on Mathematical Software*, 37(4):40.
- Lindgren, F., Rue, H., and Lindström, J. (2011). An explicit link between Gaussian fields and Gaussian Markov random fields: the stochastic partial differential equation approach. *Journal of the Royal Statistical Society: Series B*, 73(4):423–498.
- Nychka, D. W., Bandyopadhyay, S., Hammerling, D., Lindgren, F., and Sain, S. R. (2015). A multi-resolution Gaussian process model for the analysis of large spatial data sets. *Journal of Computational and Graphical Statistics*, 24(2):579–599.
- OCO-2 Science Team, Gunson, M., and Eldering, A. (2015). OCO-2 Level 2 bias-corrected solar-induced fluorescence and other select fields from the IMAP-DOAS algorithm aggregated as daily files, retrospective processing V7r. <https://disc.gsfc.nasa.gov/datacollection/OCO2.L2.Lite.SIF.V7r.html>.
- Quiñonero-Candela, J. and Rasmussen, C. E. (2005). A unifying view of sparse approximate Gaussian process regression. *Journal of Machine Learning Research*, 6:1939–1959.
- Rasmussen, C. E. and Williams, C. K. I. (2006). *Gaussian Processes for Machine Learning*. MIT Press.
- Rue, H. and Held, L. (2005). *Gaussian Markov Random Fields: Theory and Applications*. CRC press.
- Sang, H., Jun, M., and Huang, J. Z. (2011). Covariance approximation for large multivariate spatial datasets with an application to multiple climate model errors. *Annals of Applied Statistics*, 5(4):2519–2548.
- Snelson, E. and Ghahramani, Z. (2007). Local and global sparse Gaussian process approximations. In *Artificial Intelligence and Statistics 11 (AISTATS)*.
- Stein, M. L., Chi, Z., and Welty, L. (2004). Approximating likelihoods for large spatial data sets. *Journal of the Royal Statistical Society: Series B*, 66(2):275–296.
- Stroud, J. R., Stein, M. L., and Lysen, S. (2017). Bayesian and maximum likelihood estimation for Gaussian processes on an incomplete lattice. *Journal of Computational and Graphical Statistics*, 26(1):108–120.
- Sun, Y. and Stein, M. L. (2016). Statistically and computationally efficient estimating equations for large spatial datasets. *Journal of Computational and Graphical Statistics*, 25(1):187–208.
- Tzeng, S. and Huang, H.-C. (2018). Resolution adaptive fixed rank kriging. *Technometrics*.
- Vecchia, A. (1988). Estimation and model identification for continuous spatial processes. *Journal of the Royal Statistical Society, Series B*, 50(2):297–312.
- Wikle, C. K. and Cressie, N. (1999). A dimension-reduced approach to space-time Kalman filtering. *Biometrika*, 86(4):815–829.